JOURNAL OF MATERIALS SCIENCE 27 (1992) 2877–2886

Reaction-sintered hot-pressed TiAl

J. C. RAWERS, W. R. WRZESINSKI*
Albany Research Center, Bureau of Mines, Albany, OR, USA

Titanium aluminide intermetallic alloys and composites were formed from elemental titanium and aluminium powders by self propagating, high-temperature synthesis in an induction-heated hot-press. The crystal phases, density, transverse rupture stress, and hardness of the reaction-sintered compacts, were observed to be controlled by hot-pressing conditions. The principal phase formed was TiAl together with a significant second-phase concentration of Ti_3Al. The transverse rupture strength (TRS) of the intermetallic composites was observed to vary directly with compact density. Under selected high-temperature synthesis hot-pressing conditions, TRS values were comparable to those obtained for fully dense TiAl. Titanium aluminide composites were formed by adding boron, carbon, silicon and Al_2O_3, and SiC powders and whiskers to the Ti–Al powders before reaction sintering. Changing the alloying additions did not have as strong an effect on properties of the composite compacts as did varying hot-pressing conditions.

1. Introduction

Intermetallics at elevated temperatures are currently being studied for use as engineering materials. Fabricating and processing of intermetallics have included most of the conventional techniques [1–3] used with metal alloys: melt casting, powder processing, forging, etc. Recent research has shown that it is possible to produce finished, near net-shape ceramic and intermetallic products from elemental powders in a single step [4, 5].

The formation of intermetallics and intermetallic composites can be accomplished in a single-step reaction from elemental powders by self-propagating high-temperature synthesis (SHS) [6]. In the SHS process, the exothermic heat-of-formation energy cause a reaction front to propagate through a near stoichiometric composition of elemental powders producing an intermetallic alloy. Several different ceramic and intermetallic alloys, such as aluminides, borides, carbides, and silicides [7], have been prepared by SHS reactions. In a recent study [8], the thermodynamics and kinetics of the titanium–aluminium SHS reaction were determined. In other studies, the effects of varying the experimental parameters that control the SHS reaction, such as powder size and alloy composition, were investigated [5, 9]. As part of that study, a third element (boron, carbon or silicon) was added to the titanium and aluminium powder mixture. Simultaneous SHS reactions were achieved with the final synthesis reaction producing an intermetallic composite.

In this study, the fabrication of intermetallic matrix composites into a finished near net-shape product from pure elemental powders was accomplished *in situ* by reactive sintering in a hot-press (RES–HOP). In this processing technique, Ti–Al powder mixtures were placed in a graphite die of the desired shape and a mild pressure applied. The SHS reaction was initiated by heating the entire die up to the melting point of aluminium. The molten aluminium reacted with the titanium and then initiated the SHS reaction. The term "reactive sintering" is used instead of SHS because the entire powder compact was heated up so that the SHS reaction occurs throughout the sample at the same time. The pressure applied during the reactive sintering, i.e. the hot-pressing, was used to produce a nearly fully dense net-shape TiAl product. Previous attempts to form TiAl by SHS alone have met with limited success [9]. The success of forming near-fully-dense titanium aluminides results from combining the SHS reaction and hot-pressing, RES–HOP. Evaluation of the mechanical and physical properties of the RES–HOP samples included density, hardness, transverse-rupture-stress, X-ray diffraction, and metallographic and SEM–EDS analysis.

This research is part of the US Bureau of Mines programme to develop advanced materials as substitutes for metal alloys containing strategic elements.

2. Experimental procedure

Titanium aluminide composites were prepared by reaction sintering and hot-pressing elemental powders in a vacuum-induction furnace. Mechanical and physical characteristics of the compacts were then determined.

Two 500 g master mixtures of titanium and aluminium powders were prepared in a one-to-one atomic per cent composition (Ti*Al). High-purity (> 99.9%)

* *Present address*: US Department of Energy, Richland, WA, USA.

0022–2461

titanium (− 100 mesh) and aluminium (− 325 mesh) powders were blended by ball-milling with methanol for 20 h. The blended powder was then air dried for 24 h, after which the powder was placed in a low-vacuum oven to dry at 135 °C for 1 h.

Powder composite mixtures of smaller mass (approximately 15 g) were prepared by combining 2, 5, and 10 mol % additions of aluminium, boron, carbon, silicon, Al_2O_3, and SiC (both whiskers and particles) with the previously prepared Ti*Al master mixture. (Note, the measuring designation is moles rather than atomic per cent because when forming a powder composite, the Ti*Al powder mixture was considered to be the intermetallic compound TiAl and, while the elemental additions, aluminium, boron, carbon and silicon could be designated in atomic percentage, the quantity of Al_2O_3 and SiC added can be best expressed in mole per cent.) Duplicate samples of the 5 mol % compositions were made to evaluate sample and experimental reproducibility. The composite powder mixtures were lightly ground in a mortar and pestle for several minutes. They were then placed in plastic vials along with several ceramic balls and shaken for 10–15 min. Examination of the blended powders with an optical microscope showed a uniform powder composition and little or no change in the powder resulting from the mechanical blending. The powders were then poured into graphite dies for hot pressing.

The hot-pressing was conducted in a vacuum (10^{-3}–10^{-4} torr; 1 torr = 1.333×10^2 Pa) induction furnace. While at room temperature, a uniaxial stress load (6.5 MPa) was applied. The temperature was monitored using an optical pyrometer. Maximum hot-press temperature was approximately 1300 °C. In addition to the time required for heating the samples, normally about 10 min, each sample was sintered for various times at the maximum temperature and pressure. Compaction of the powder was monitored by movement of the loading of the die plunger. The original size of the RES–HOP samples was 2.0 cm diameter and approximately 2.5–3.5 cm high.

Three different series of experiments were conducted to characterize the effects of varying the hot-pressing conditions. In the first series, the compaction pressure was 6.5 MPa and the maximum hot-pressing temperature was varied between 900 and 1300 °C. In the second series, the maximum temperature was 1300 °C and the pressure was varied between 6.5 and 13 MPa. In the third series, the sintering pressure and temperature were 6.5 MPa and 1200 °C, respectively, and the processing time was varied between 15 and 180 min.

After hot-pressing, the samples were removed from the graphite dies and machined to remove any products that may have resulted from surface reaction with the graphite die. Bulk density of the machined samples was then determined using the measured weight and apparent total volume.

X-ray diffraction patterns of the machined surfaces were used to determine the phases present in the reaction product. The relative quantities of the different titanium aluminides (TiAl and Ti_3Al) present were determined by comparing the X-ray intensity peaks of the TiAl (2 0 0) and the Ti_3Al (1 1 0) planes. References powder diffraction patterns for these compositions indicated that the relative intensity of both of these peaks is 60% that of the maximum peaks. The maximum intensity peaks for the individual compounds could not be used because there were interference peaks nearby. The relative ratio of the two aluminides, TiAl: Ti_3Al, is reported.

The hot-pressed samples were sliced with a diamond saw into several discs, each 3–5 mm thick, and polished to a 600 grit finish for transverse-rupture-stress (TRS) tests. TRS tests followed the general experimental description outlined in ASTM-B 528. The centre span was 10 mm and the support width was 12 mm. Computer-simulated analyses using finite element analysis have shown that for these test conditions and sample size, there is no significant difference in TRS test results between rectangular plates and cylindrical discs [10]. A scanning electron microscope (SEM) was used to examine a fracture surface from each TRS sample. The other half of the TRS specimen was mounted, polished, and examined to determine its microstructure. After fracture testing, Rockwell hardness values, R_a, were obtained.

3. Results

Reaction sintering/hot-pressing (RES–HOP) of titanium and aluminium elemental powder mixture (Ti*Al) resulted in the formation of two titanium–aluminium intermetallic phases, TiAl and Ti_3Al, together with selected precipitates depending upon the alloy addition. During hot-pressing it was observed that over 90% of the compaction occurred during heat-up at approximately 665 °C. In previous reactive-sintering studies with Ti*Al [10], differential scanning calorimetry showed several strong exothermic reactions after the powder compacts reached the melting point of aluminium ($T_{m.p.}$ 665 °C). This was attributed to the SHS reactions

$$Ti + Al \rightarrow TiAl \quad (1)$$

$$TiAl + 2Ti \rightarrow Ti_3Al \quad (2)$$

resulting in the two intermetallic phases observed in X-ray diffraction.

The results of multiple runs of Ti*Al, the effects of varying hot-pressing conditions, and the effects of adding alloying elements to Ti*Al are presented below. The results of each Ti*Al composite are discussed separately.

3.1. Ti*Al duplicates

To characterize the mechanical and physical properties and to evaluate reproducibility, 15 different Ti*Al samples were prepared (Table I). Hot-pressing conditions were identical for each test: 1300 °C, 6.5 MPa, and 5 min processing time. There was less than 5% variation in the bulk densities and hardness measurement between samples. The 5% variation includes variations in sample preparation, i.e. powder mixing,

TABLE I Mechanical and physical properties of Ti*Al (the table has been arranged in order of increasing density). Hot-pressing conditions: 1300 °C, 6.5 MPa, and 5 min processing time

Sample	Density ($g\,cm^{-3}$)	Phase concentration[c] ($TiAl/Ti^3Al$)	Hardness (R_a)	TRS[a] (MPa)
a	3.21	2.3	48	178, 235
b	3.27	2.0	52	306, 335
c	3.34	2.9	–	281, 351, 463
d	3.41	1.8	60	269, 291
e	3.44	1.8	58	331, 408
f	3.46	2.8	62	285, 300
g	3.49	3.6	–	341, 403, 433
h	3.51	1.6	61	390, 489
i	3.51	3.1	62	425, 590
j	3.53	1.8	64	280, 370
k	3.53	3.5	62	240, 495
l	3.55	2.2	59	346, 374
m[b]	3.56	6.1	–	296, 510, 510
n	3.59	4.0	62	350, 360
o	3.67	5.2	–	415, 458
Average	3.50	2.5	61.1	368
S.D.	± 0.06	± 0.8	± 1.8	± 15

[a] Each hot-pressed sample was divided into two or three TRS samples.
[b] Both titanium and aluminium powders were − 325 mesh.
[c] Determined from ratio of X-ray diffraction peaks.

hot-pressing, and machining. The theoretical density of TiAl is $3.83\,g\,cm^{-3}$. The observed density was $3.50\,g\,cm^{-3}$ or approximately 91% full density.

X-ray analysis showed only two phases to be present: TiAl and Ti_3Al (Fig. 1). The ratio of TiAl to Ti_3Al showed that the dominant phase was TiAl. However, there was a significant quantity of Ti_3Al present, typically 25%–30%. When different sections of the same hot-pressed sample were analysed, X-ray data showed that the middle region of the compacts had a higher $TiAl/Ti_3Al$ ratio, 10 (± 30%), than the top or bottom regions, 3 (± 125%). The X-ray data reported in Tables I, II and III represent average values obtained from the top and bottom of the cylinder. The width of the diffraction lines also varied with respect to different regions of the sample. Sharper lines, associated with larger grains, were obtained in the centre region. Broader lines, associated with grains approximately 100 nm diameter, were obtained from the outer regions.

Microprobe analysis showed that the composition of the Ti_3Al structure was much less than 75 at % Ti, and the TiAl structure was also less than 50 at % Ti (Fig. 2).

Transverse-rupture-stress (TRS) results of a total of 33 fracture tests obtained from 15 different samples showed significant variation in failure loads. The most appropriate statistics for this type of failure analysis are the "weak link", or Weibull, statistics. Weibull statistical analysis gave a mean TRS of 368 MPa (± 15.4) and a shape factor of 4.25 (± 0.69) (Fig. 3). A shape factor of 3.44 indicates a Gaussian curve. Grinthal [11] reported TRS values of 793 MPa for fully dense TiAl. The observed reduction in TRS values was attributed to internal cracks or voids present and associated with the porosity.

Scanning electron microscope–EDX examination of cross-sectioned and metallographically polished samples showed the presence of two titanium–aluminium intermetallic phases with large differences in chemical composition (Fig. 1). The matrix (the darker regions in the photograph) was identified by microprobe analysis (Fig. 4) to be TiAl and the precipitate (the lighter region) within the matrix was identified to be Ti_3Al. SEM examination showed numerous voids located principally in the TiAl phase (Fig. 1).

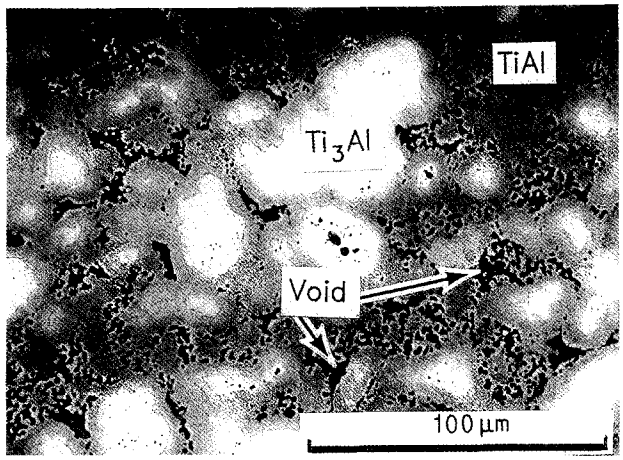

Figure 1 SEM backscattered photograph of hot-pressed Ti*Al. Light regions are Ti_3Al. Continuous grey region is TiAl. Note numerous small voids located primarily in the TiAl phase.

Examination of the scanning electron micrographs suggests that the synthesis reaction initiated at many different locations simultaneously. (If there was only a single point of initiation, the pressure would tend to eliminate formation of voids along the reaction front.) The aluminium melted in different microregions initiating the Ti–Al synthesis reaction. Eventually the reaction fronts coalesced and welded together. The voids appear to have formed during the synthesis reaction.

TABLE II Mechanical and physical properties of Ti*Al as functions of hot-pressing conditions

(a) Processing conditions: temperature varied, loading pressure 6.5 MPa and sintering time 15 min

	Temperature (°C)				
	900	1000	1100	1200	1300
Density (g cm^{-3})	3.21	3.27	3.40	3.45	3.54
X-ray ($TiAl/Ti_3Al$)	0.71	0.88	1.3	1.8	2.3
Hardness, R_a	55	59	60	60	58
TRS ⟨average⟩	⟨149⟩	⟨206⟩	⟨248⟩	⟨280⟩	⟨378⟩
(MPa)	130–168	192–221	242–254	269–291	358–398

(b) Processing conditions: loading pressure varied, maximum temperature 1300 °C and sintering time 15 min

	Pressure (MPa)	
	6.5	10
Density (g cm^{-3})	3.50	3.75
X-ray ($TiAl/Ti_3Al$)	2.5	1.53
Hardness, R_a	61	57
TRS ⟨average⟩	⟨366⟩	⟨801⟩
(MPa)	354–378	727–876
		799

(c) Processing conditions: sintering time varied maximum temperature 1200 °C and loading pressure 6.5 MPa

	Time (min)		
	15	60	180
Density (g cm^{-3})	3.49	3.64	3.78
X-ray ($TiAl/Ti_3Al$)	2.9	1.9	5.4
Hardness, R_a	61	66	58
TRS ⟨average⟩	⟨415⟩	⟨637⟩	⟨1115⟩
(MPa)	404–425	630–643	1108–1122

TABLE III Mechanical and physical properties ot Ti*Al composites alloyed with aluminium, boron, carbon, silicon Al_2O_3, SiC_P (particles), and SiC_W (whiskers)

		Composition						
		Al	B	C	Si	Al_2O_3	SiC_P	SiC_W
Density	0	3.50	3.50	3.50	3.50	3.50	3.50	3.50
(g cm^{-3})	2	3.52	3.45	3.55	3.43	3.37	3.27	3.40
	5	3.61	3.37	3.45	3.46	3.20	3.40	3.13
		3.46	3.41	3.49	3.65	3.09	3.54	3.02
	10	3.55	3.30	3.33	3.41	3.05	3.53	3.91
X-ray	0	2.45	2.45	2.45	2.45	2.45	2.45	2.45
(TiA/Ti_3Al)	2	4.0	2.8	1.3	3.7	2.4	3.3	3.0
	5	3.2	3.8	1.7	3.7	7.1	4.1	4.1
		2.4	3.3	4.2	4.5	4.2	3.4	4.1
	10	2.5	2.2	2.5	4.2	3.5	8.3	7.6
Hardness, R_a	0	61.1	61.1	61.1	61.1	61.1	61.1	61.1
	2	62	63	57	61	55	57	58
	5	64	59	58	64	47	59	45
		62	62	58	69	48	61	41
	10	66	62	53	63	40	52	25
TRS*	0	368	368	368	368	368	368	368
MPa	2	410	370	325	340	242	307	304
		420	410	450	380	254	367	316
	5	380	320	280	290	214	307	257
		480	320	305	422	218	263	261
		320	310	365	380	166	224	214
		480	340	375	450	203	289	226
	10	290	240	225	215	161	157	161
		460	370	315	301	213	206	97

* Each sample was divided into two TRS samples.

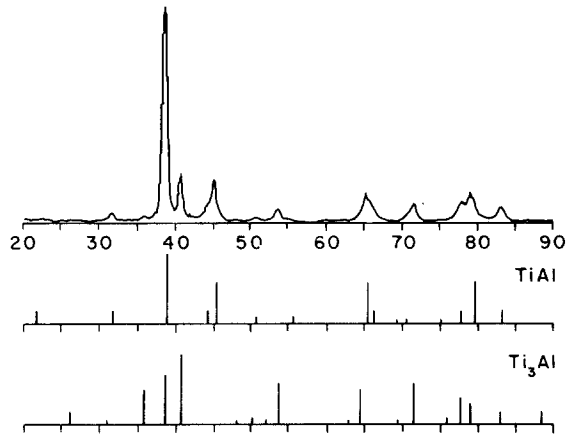

Figure 2 X-ray diffraction analysis of hot-pressed Ti*Al.

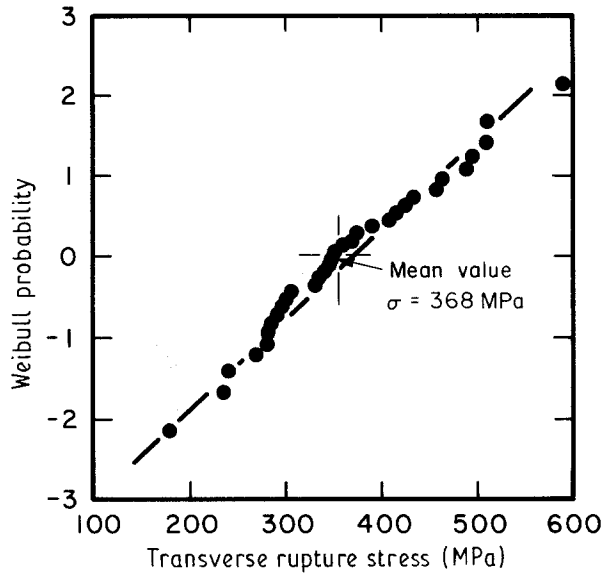

Figure 3 Weibull probability plot of transverse-rupture-stress.

Compaction pressures were insufficient to consolidate completely the products.

Scanning electron microscope examination of fracture surfaces showed the presence of two different fracture patterns (Fig. 5): (i) a relatively smooth, flat, and somewhat wavy, brittle failure that occurred through the Ti_3Al crystal structure and, (ii) a more meandering, but still brittle, fracture pattern that was associated with the fracture connecting the cracks and voids in the TiAl structure. There was little indication of any ductile fracture. The fracture propagated across the sample, passing smoothly between the two different titanium–aluminium phases. There appeared to be strong interface bonding between the TiAl and the Ti_3Al.

In a separate experiment, powders of equal size (i.e. − 325 mesh), were used to fabricate Ti*Al (Table I, Sample M).

3.2. Ti*Al hot pressing

3.2.1. Temperature

A series of Ti*Al samples were hot-pressed with maximum sintering temperature varying between 900 and 1300 °C. The density and the TRS values for these samples increased approximately linearly with increasing temperature (Table II). There was no appreciable change in hardness. SEM examination of metallographically polished samples showed that changing the sintering temperature altered the Ti_3Al microstructure (Fig. 6). The higher the temperature, the greater the amount of TiAl formed. At the lower temperatures, large voids occurred in the centre of the Ti_3Al regions. As the sintering temperature increased, these voids closed.

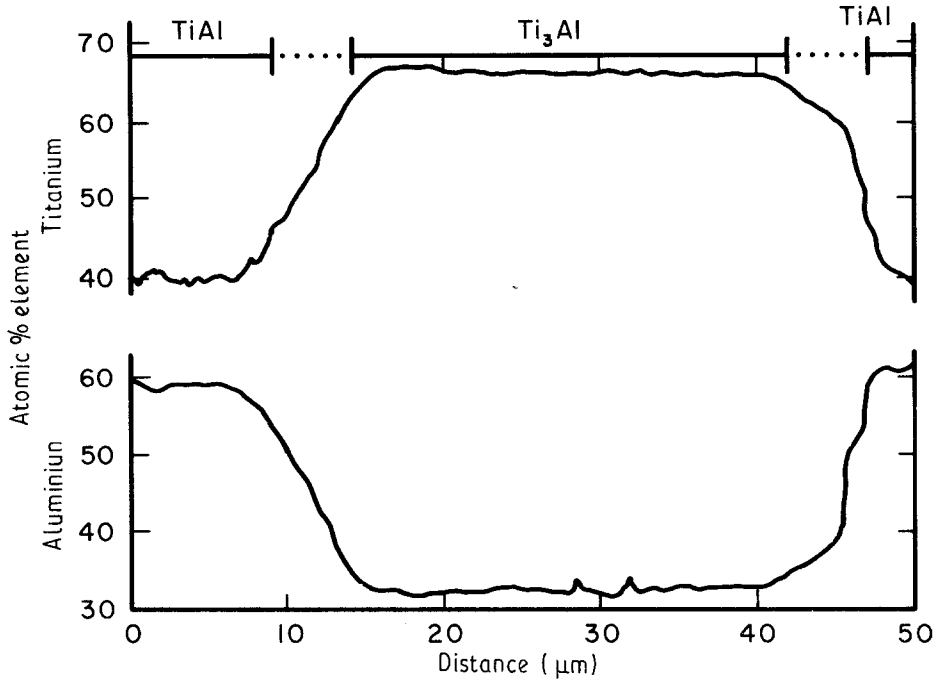

Figure 4 Microprobe analysis of hot-pressed Ti*Al. Line analysis across two grains identified by X-ray analysis and microprobe to be TiAl and Ti_3Al.

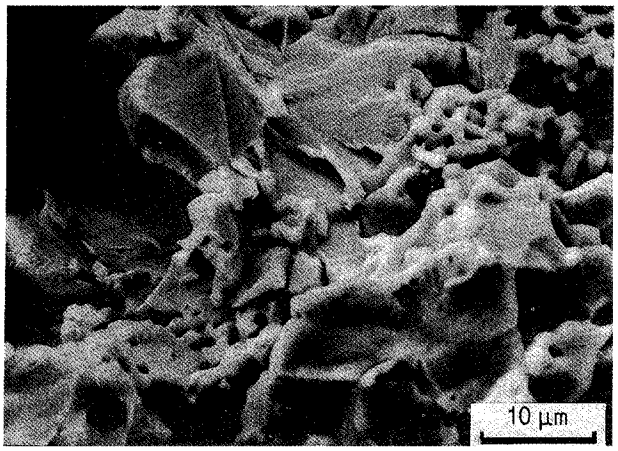

Figure 5 SEM fracture pattern of hot-pressed Ti*Al. Fractures across Ti_3Al are relatively flat. Fractures across TiAl have sponge-like appearance.

3.2.2. Ti*Al hot-pressing pressure

In the second Ti*Al series, the maximum hot-pressing stress was varied between 6.5 and 27.5 MPa. However, only the 6.5 and 10 MPa tests were considered valid runs. For the higher pressure runs, especially at 20 and 27.5 MPa, the graphite dies broke during hot-pressing and liquid aluminium was squeezed out.

For these samples, the density and TRS values increased with increasing pressure. The maximum TRS value of 801 MPa occurred with a maximum loading force of 10 MPa. As previously noted, the TRS value obtained by Grinthal [11] for pure TiAl was 790 MPa. The phase morphology of the TiAl–Ti_3Al grains changed significantly with different pressures (Fig. 7). SEM examination of the fracture surface showed that the increase in TRS is related to a decrease in TiAl porosity. Further refinement of the hot-pressing loading conditions and strengthening of the graphite dies could possibly increase the fracture strength significantly above that obtained for pure TiAl.

3.2.3. Ti*Al hot pressing-time

In a third series used Ti*Al, the maximum hot-pressing temperature, 1200 °C, and pressure, 6.5 MPa, were held constant and the total hot-pressing processing time was varied between 15 and 180 min (Table II). Density increased with increasing sintering time, approaching the TiAl theoretical density of 3.83 $g\,cm^{-3}$. The increase in TRS values with time closely matched the increase in density with time (Fig. 8). The TRS values obtained for the 180 min sintering time were significantly above those reported for pure meltcast TiAl [11]. Results of the TRS data indicate that a TiAl/Ti_3Al composite structure (Fig. 9) may be beneficial as opposed to a single phase. SEM examination shows a transition of grain morphology with sintering time from an open, porous structure for short sintering times, to a classical, equiaxial, almost fully dense grain structure for the longer times.

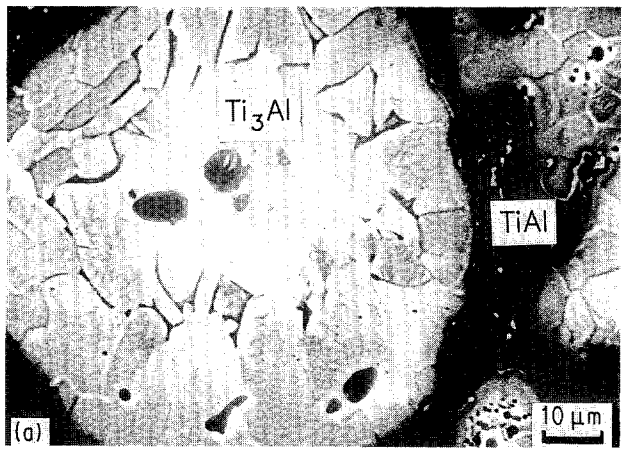

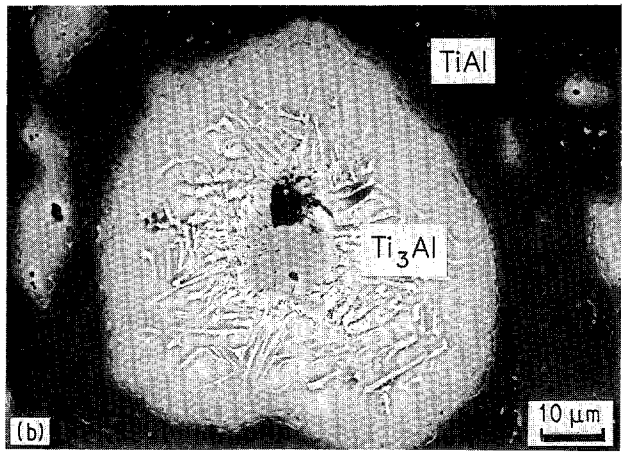

Figure 6 SEM backscattered photograph of hot-pressed samples – temperature varied. Ti_3Al phase. (a) 900 °C, (b) 1100 °C.

3.3. Ti*Al summary

Fig. 10 shows a linear relationship between density and maximum sintering time, temperature, and TRS and sintering temperature. It is obvious that TRS is directly related to sample density. A summary of all data is presented in Fig. 10.

3.4. Ti*Al composites *in situ*

Four different elemental powders, aluminium, boron, carbon and silicon, were added to the Ti*Al powder mixture at several concentrations (2, 5 and 10 mol %) (Table III). The experimental RES–HOP conditions were held constant, i.e. maximum temperature 1300 °C, pressure 6.5 MPa, and processing time 15 min. The additional alloying with aluminium was intended to evaluate the effect of increasing the amount of molten metal present during the initial phase of the reaction-sintering process. Boron, carbon, and silicon powders were added so that during the SHS reaction, titanium would form additional intermetallic phases that are more stable than TiAl. The addition of boron, carbon or silicon would produce a second intermetallic phase in addition to Ti*Al and can be thought of as simultaneous SHS reactions that forms titanium aluminides in combination with titanium borides, carbides, or silicides. The final product would be an intermetallic composite formed *in situ* from elemental powders. The extended TiAl solubility

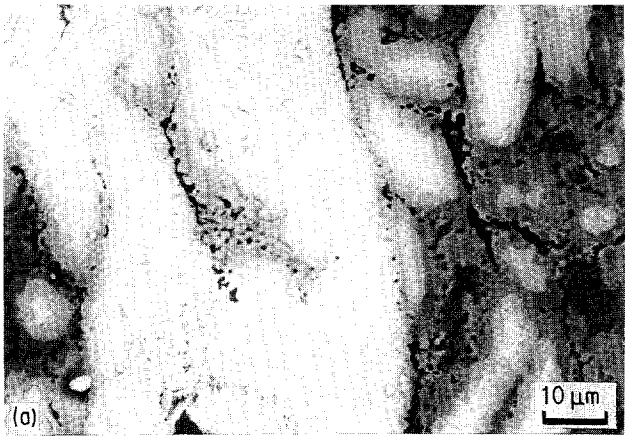

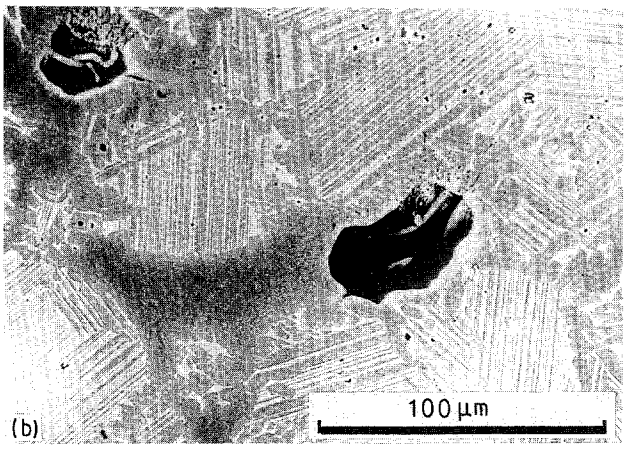

Figure 7 SEM backscattered photograph of hot-pressed samples – pressure varied. Ti_3Al phase: (a) 6.5 MPa, (b) 10 MPa.

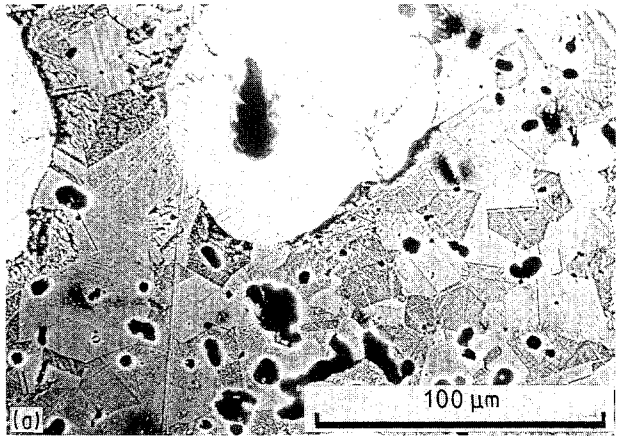

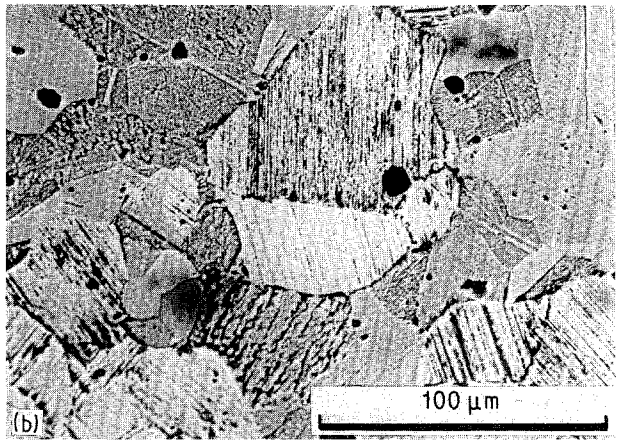

Figure 9 SEM backscattered photograph of hot-pressed samples – time varied. Ti_3Al phase: (a) 1 h, (b) 3 h.

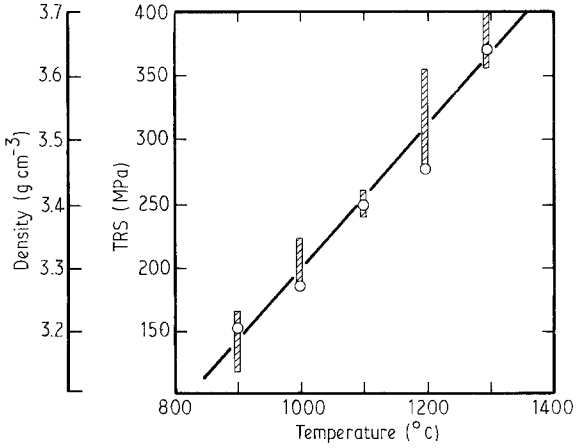

Figure 8 Variation of hot-pressing density (○) and TRS values (cross hatched) with temperature.

range ensured that, theoretically, only TiAl and the composite should form.

3.4.1. Aluminium

Addition of aluminium (2, 5 and 10 mol %) to Ti*Al did not have a significant effect on the mechanical and physical properties of reaction-sintered compacts (Table III). No significant change in bulk densities occurs with a change in aluminium concentration.

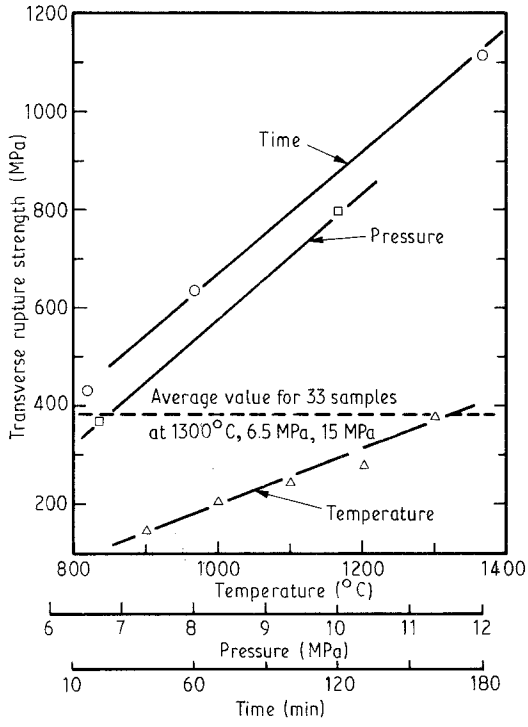

Figure 10 Density and transverse-rupture-stress data as a function of RES–HOP experimental variables; temperature, pressure and time.

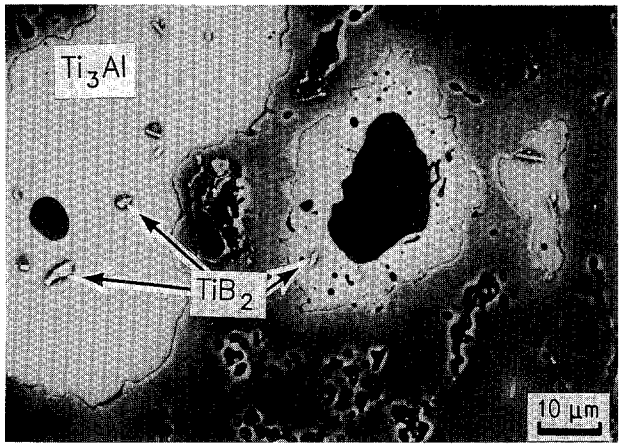

Figure 11 SEM backscatterd photograph Ti*Al–5 mol % B composite. TiB_2 precipitates located inside the Ti_3Al (light region).

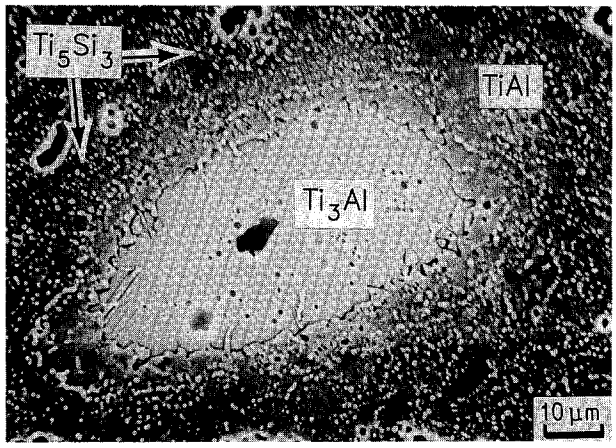

Figure 13 SEM backscattered photograph of Ti*Al–5 mol % Si composite. Ti_5Si_3 precipitates located within TiAl and on void-surface interface.

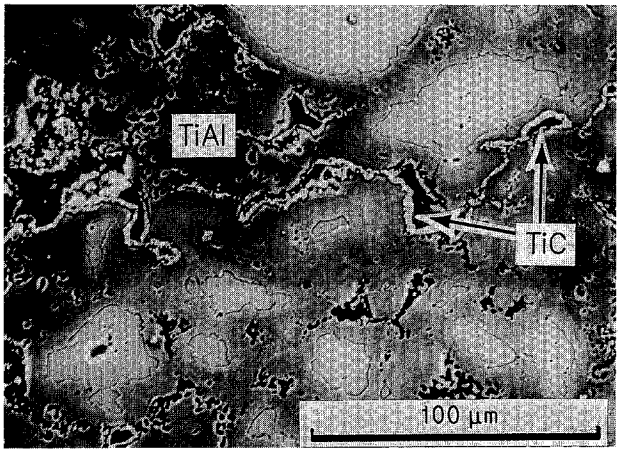

Figure 12 SEM backscattered photograph of Ti*Al–5 mol % C composite. TLC continuous phase located on the void–Ti_3Al interface (bright white region).

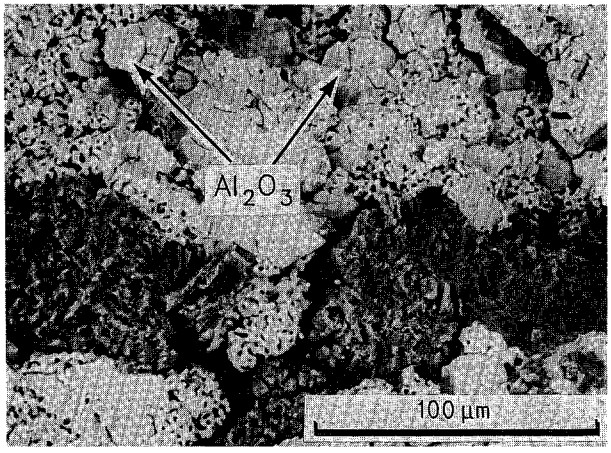

Figure 14 SEM backscattered photograph of Ti*Al–5 mol % Al_2O_3 composite. Al_2O_3 particles (darker regions) are embedded within TiAl–Ti_3Al (lighter regions).

There was a small but statistically significant increase in hardness with increasing aluminium concentration and the TRS values decreased slightly. Examination of the fracture surface showed failure features similar to those observed for the Ti*Al series described previously.

3.4.2. Boron

Addition of boron (2, 5 and 10 mol %) to Ti*Al decreased bulk density and TRS values. There was no significant change in hardness (Table III). SEM analysis of the metallographically polished surfaces showed the presence of a fine precipitate in the Ti_3Al phase that was identified by X-ray diffraction to be TiB_2 (Fig. 12). Examination of the fracture surface indicated that the TiB_2 precipitates did not influence fracture morphology.

3.4.3. Carbon

The addition of carbon (2, 5 and 10 mol %) to Ti*Al decreased bulk density, decreased TRS values, and decreased hardness (Table III). The Ti*C SHS reaction product was observed by SEM and identified by X-ray diffraction to be TiC. SEM–EDX analysis showed that the reaction produced a thin second-phase film on the surface of the TiAl matrix (Fig. 13). The morphology of the fracture surface did not suggest that the presence of a continuous carbide layer on the TiAl surface influenced the failure.

3.4.4. Silicon

The addition of silicon (2, 5 and 10 mol %) to Ti*Al had little effect on density and hardness. TRS values were quite scattered but showed a decreasing trend with increasing silicon concentration (Table III). SEM–EDX analysis showed that the SHS Ti*Si reaction produced a fine precipitate within and on the Ti_3Al grain surface (Fig. 14). The reaction product of silicon and Ti*Al was identified by X-ray diffraction to be Ti_5Si_3 (Fig. 15). Fracture morphology showed that the Ti_5Si_3 precipitate did not influence failure.

3.5. Ti*Al composite

Al_2O_3 and SiC particles were added to the Ti*Al before RES–HOP to form intermetallic composites *in situ*. It was hoped that during the Ti–Al synthesis the

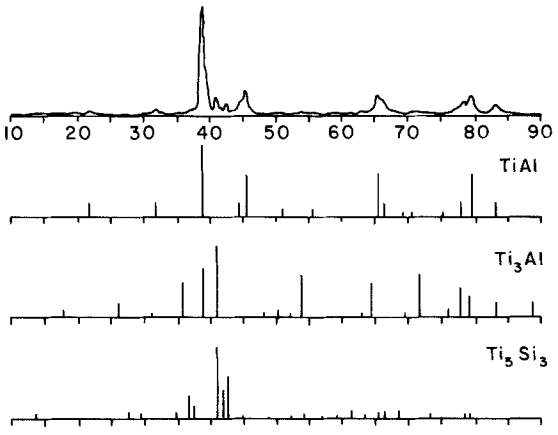

Figure 15 X-ray diffraction pattern of Ti*Al–5 mol % Si composite.

Al_2O_3 and SiC would become part of the microstructure and form a structurally sound composite.

3.5.1. Ti*Al–Al_2O_3 composite

Addition of Al_2O_3 (2, 5 and 10 mol %) to Ti*Al had a significant effect in reducing density, hardness, and TRS values of the composite almost linearly with increase of Al_2O_3 concentration. X-ray diffraction showed the presence of only TiAl, Ti_3Al, and Al_2O_3. Neither X-ray diffraction nor SEM analysis showed any indication of an interaction, a reaction, or any bonding between the Al_2O_3 powder addition and titanium aluminides. As a result of the lack of interaction or bonding, the Al_2O_3 particles acted as internal voids or cracks (Fig. 15) in decreasing the TRS values.

3.5.2. Ti*Al–SiC (particles and whiskers) composite

Addition of SiC (2, 5 and 10 mol %) to Ti*Al had similar effects on the mechanical and physical properties as the addition of Al_2O_3. (Table III) TRS values decreased with increasing SiC concentration. This was especially obvious with the addition of SiC whiskers. SEM examination showed that a reactant phase formed at the SiC–TiAl interface. X-ray diffraction identified this phase as Ti_5Si_3. For larger SiC concentrations, much of the SiC appeared to be grouped together into small clusters (Fig. 16). This suggests that when the aluminium melts, and the SHS reaction proceeds, the SiC particles float on the liquid aluminium surface, and the individual molten aluminium regions coalesce bring the SiC particles together into small clusters with a void at the centre.

3.5.3. Ti*Al composite–summary

Additions of a third element to Ti*Al can result in simultaneous SHS reaction and produce an intermetallic composite. The microstructure of the composite depends on the element added. Increasing the concentration of the third element did not reduce the porosity but decreased the resulting mechanical properties.

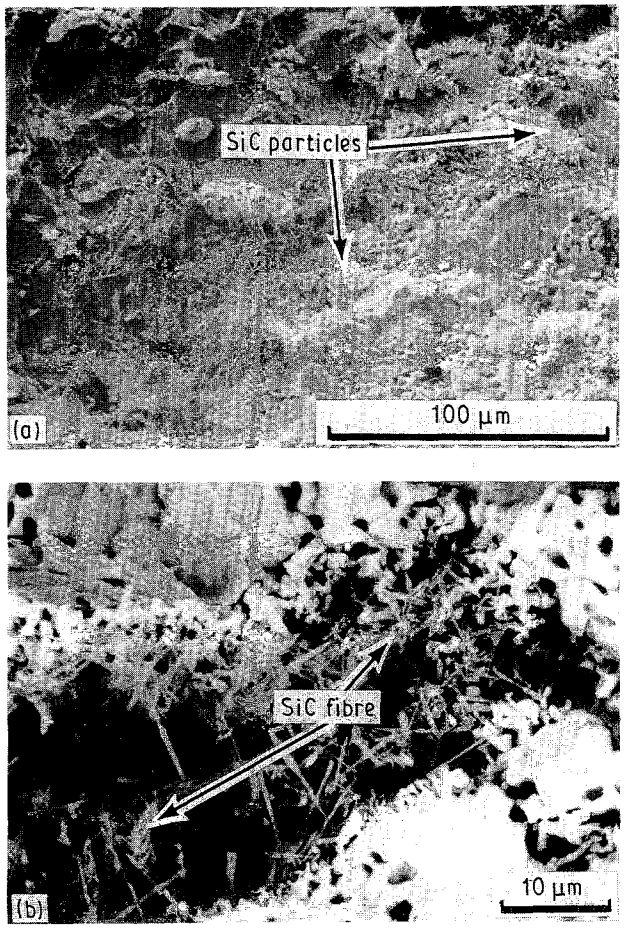

Figure 16 SEM backscattered photographs of Ti*Al–5 mol % SiC composite. SiC whiskers located in voids adjacent to TiAl phase.

4. Discussion

Two different titanium aluminide phases, TiAl and Ti_3Al, were produced in different ratios depending on the powder mixture composition and the hot-pressing conditions. The reaction-sintering process started with the compaction of powders at the melting temperature of aluminium at 665 °C [9]. The most probable sequence of events consistent with the data is that the liquid aluminium flowed around the titanium powder and started the $Ti + 3Al \rightarrow TiAl_3$ reaction. This Ti–Al SHS reaction is extremely exothermic and heated the local material above the melting point of $TiAl_3$. At this point the remaining titanium reacted as $2Ti + TiAl_3 \rightarrow 3TiAl$. This reaction is also exothermic. Thus, the local temperature of the SHS front could be above 1460 °C, the melting temperature of TiAl.

For a 50–50 Ti*Al atomic per cent composition, the phase diagram show two different crystal phases may be present depending upon the temperature [12]. At elevated temperatures, from approximately 1400–1460 °C, it is possible for the stoichiometric Ti–Al composition to form the crystal phase associated with Ti_3Al, DO_{19} (ordered hexagonal). As the alloy cools below approximately 1350 °C, the same stoichiometric composition forms the crystal structure associated with TiAl, $L1_0$ (ordered face-centred-tetragonal). For all temperatures, both TiAl and Ti_3Al phases have solubility ranges that extend to approximately ± 10 at % off stoichiometry.

In a typical SHS reaction, the powder reaction is initiated at room temperature. In reaction sintering, the Ti*Al powder is preheated to an elevated temperature, which in this case is the melting temperature of aluminium. The exothermic energy previously used to heat the powder ahead of the synthesis reaction front in the SHS reaction is now used in the RES–HOP process to superheat the titanium aluminide above its melting point and allow the high-temperature TiAl and Ti_3Al phases to form.

The amount of Ti_3Al produced depends upon the exothermic energy released and the heat treatment following its formation.

By controlling the reaction-sintering hot-pressure processing conditions, it is possible to control the sample density, transverse-rupture-stress, that is directly related to the density, and the TiAl/Ti_3Al phase ratio. Density can be increased slightly with increasing maximum temperature and increased significantly by increasing the pressure and/or sintering time. The TRS is directly related to the density, regardless of how the density was obtained. The TiAl/Ti_3Al phase ratio increased with increasing sintering time and higher temperatures.

Reaction sintering of Ti*Al powders can be augmented by the addition of small quantities of elemental powders that will react with either titanium or aluminium and form a more stable intermetallic phase than either TiAl or Ti_3Al. As a result of mixing either boron, carbon or silicon with Ti*Al and reaction sintering, two SHS reactions occurs spontaneously *in situ*. This results in the formation of a third intermetallic phase, i.e. titanium boride, carbide, or silicide precipitate, along with and generally associated with one of the two titanium aluminide phases, TiAl or Ti_3Al. Each different intermetallic composite has its own unique microstructure. The titanium diboride precipitate formed within the Ti_3Al. Titanium carbide formed a continuous third phase layer on the outside surface of the TiAl. Titanium silicide formed a precipitate within the TiAl.

Small concentrations of alloying elements did not significantly change the physical properties of the SHS composites. Larger concentrations, however, did adversely affect the TRS.

In a second effort to form SHS intermetallic composites, Al_2O_3 and SiC powders were added to Ti*Al before reaction sintering. Al_2O_3 particles did not react with, nor interact with, the titanium aluminides formed during reaction sintering. On the other hand, SiC particles and whiskers did react with the titanium aluminides.

All of the composites were formed under experimental conditions that produced a significant quantity of voids. Alloying did not affect the void density or distribution. Hot-pressing conditions can reduce void density through increased reaction temperature, time, or load pressure. Increasing the load significantly decreased the void concentration and drastically increased the TRS strength.

5. Conclusion

Formation of intermetallic composites with Ti*Al can be accomplished by reaction sintering–hot pressing. The mechanical and physical properties of reaction-sintered Ti*Al were strong functions of hot-pressing conditions. Reaction sintering–hot pressing can produce TRS values equal to those of fully dense materials. Intermetallic composites were formed *in situ* by adding fibres or particles or by alloying elements to the Ti*Al powder and initiating the exothermic SHS reaction. Some mechanical and physical properties could be altered by varying the alloy composition but not to the same extent as by varying the hot-pressing conditions.

References

1. V. K. SIKKA, "MRS Symposium Proceedings", edited by N. S. Stoloff, C. C. Koch, O. T. Liu and O. Izumi (Materials Research Society, Pittsburgh, PA, 1987) pp. 487–93.
2. D. ALMAN, J. MURRY, P. KORINKO, R. ODDONE and N. S. STOLOFF, "Powder Processing of High Temperature Intermetallic Alloys", presented at the MRS annual meeting, February 1989, Las Vegas, NV.
3. A. K. GOSH, "High Temperature Processing of Titanium Alloys and Intermetallics", *ibid.*
4. W. F. HENSHAW, A. NIILER and T. LEETE, *Ceram. Eng. Sci. Proc.* **4** (1983) 634.
5. A. BOSE, B. MOORE, R. M. GERMAN and N. S. STOLOFF, *J. Metals* September **8** (1988) 14.
6. K. A. PHILPOT, Z. A. MUNIR and J. B. HOLT, *J. Mater. Sci.* **22** (1987) 159.
7. W. L. FRANKHOUSER, K. W. BRENDLEY, M. C. KIESZEK and S. T. SULLIVAN, "Gasless Combustion Syntheses of Refractory Compounds" (Noyer, Park Ridge, NJ, 1985).
8. J. C. RAWERS and W. R. WRZESINSKI, E. K. RAEB and R. R. BROWN, *Mater. Sci. Technol.* **6**(2) (1990) 187.
9. R. ODDON and R. M. GERMAN, *Adv. Powder Metall.* **3** (1989) 475.
10. W. R. WRZESINSKI and J. C. RAWERS, *J. Mater. Sci. Lett.* **9** (1990) 432.
11. R. D. GRINTHAL, in "Mechanical Properties of Intermetallic Compounds", edited by J. H. Westbrook (Wiley, New York, 1960) p. 340.
12. T. LYNAN (ed.) "Metals Handbook", Vol. 8, 8th Edn (American Society for Metals, Metals Park, OH, 1973) p. 264.

Received 26 November 1990
and accepted 10 April 1991